This is a post-peer-review, pre-copyedit version of an article published in ***Microchimica Acta*** volume 187, Article number: 638 (2020). The final authenticated version is available online at: https://doi.org/10.1007/s00604-020-04625-9

Imidazole-based ionogel as room temperature benzene and formaldehyde sensor

Nerea Gil-González[1,2]&F. Benito-Lopez[3]&E. Castaño[1,2]&Maria C. Morant-Miñana[4]

Abstract

A room temperature benzene and formaldehyde gas sensor system with an ionogel as sensing material is presented. The sensing layer is fabricated employing poly(N-isopropylacrylamide) polymerized in the presence of 1-ethyl-3-methylimidazolium ethylsulfate ionic liquid onto gold interdigitated electrodes. When the ionogel is exposed to increasing formaldehyde concentrations employing N_2as a carrier gas, a more stable response is observed in comparison to the bare ionic liquid, but no difference insensitivity occurs. On the other hand, when air is used as carrier gas the sensitivity of the system towards formaldehyde is decreased by one order of magnitude. At room temperature, the proposed sensor exhibited in air higher sensitivities to benzene, at concentrations ranging between 4 and 20 ppm resulting, in a limit of detection of 47 ppb, which is below the standard permitted concentrations. The selectivity of the IL towards HCHO and $C_6H_6$is demonstrated by the absence of response when another IL is employed. Humidity from the ambient air slightly affects the resistance of the system proving the protective role of the polymeric matrix. Furthermore, the gas sensor system showed fast response/recovery times considering the thickness of the material, suggesting that ionogel materials can be used as novel and highly efficient volatile organic compounds sensors operating at room temperature.

Keywords: Volatile organic compounds. Ionic liquid. Electrochemical gas sensor. Ionogel

Introduction

Air quality is a vibrant research area since global health organizations, and government agencies are alerting of the negative effects of the pollutants present in air over human

population and ecosystems. Volatile organic compounds(VOCs) are common air pollutants released by most of the chemical and petrochemical industries. These substances are typically present in low concentrations in air but their high volatility give them toxic properties that may affect the growth of plants and the health of humans and animals [1].Specifically, formaldehyde (HCHO) and benzene (C_6H_6)are classified as carcinogenic to humans by the International Agency for Research on Cancer [2] and one of the biggest causes of respiratory diseases. In addition to industries and traffic-related fumes, HCHO and C_6H_6canbereleasedfromseveral indoor sources such as building materials, paper walls, pressed wood, furniture, gas stoves, and cleaning or painting products been identified as the major cause of sick building syndrome. The World Health Organization (WHO) Air Quality Guideline for Europe [3] has set a 30-min exposure limit of 80 ppb for HCHO. Even though, there is not a known threshold for the risks of C_6H_6exposure, it is recommended to reduce its indoor expose as much as possible to avoid the development of cancer. There is a strong interest coming from the gas sensing market to innovate in areas related to human healthcare and environment. In particular,

high quality research is carried out towards the generation of sensors of smaller volumes, fabri cated at low cost, compact, and with lower power consumptions. Current detection technologies of VOCs are based on electronic nose sensors that can detect, quantify, and discriminate the profile of volatile compounds [4]. These devices use an array of chemical sensors that can be categorized according to their working principle: electronic noses with chemoresistive gas sensors based on carbon nanotubes(CNTs) [5], metal oxide semiconductors [6], or polymers[7]. CNT-based chemosensors present high sensitivity at room temperature due to their great adsorptive capacities, large surface-area-to-volume ratios and quick response times that significantly changes the electrical properties of the CNTs, making them promising materials for high-sensitive gas sensors for alcohol, NH3,CO2, and NOx. To enhance their sensitivity and selectivity to certain gases, they can be combined with other sensing materials such as metal oxide semiconductors. Low cost and high sensitivity are the main advantages of transition-metal oxide semiconductors (TiO2,V2O5,WO3,SnO2, and ZnO) as sensing materials. However, the high sensitivity is mainly based on the high working temperature (above 200–250 °C) at which oxygen starts to be activated. These sensors demand more cost and complicated configurations compared to others working at room temperature, which restricts their development, as a result, we have high costs of the sensor manufacture and maintenance and long-term stability problems [8]. Polymer-based gas sensing materials are widely used to detect VOCs (alcohols, aromatic compounds, or halogenated compounds). Their working principle is based on a change in the physical properties of the polymer upon gas absorption and occurs at room temperature. The electrical properties of conductive polymers are affected when exposed to diverse gases. Nevertheless, the conductivity of pure polymers is far below from the minimum required to act as gas sensors. Therefore, different processes such as doping with compounds to produce redox reactions or protonation are required to improve their conductivity at room temperature, which make them promising alternatives for future sensors[9]. Unfortunately, polymer gas sensors suffer from long-time instability, irreversibility, and poor selectivity, so the development of cheaper, simpler, and temperature independent sensing materials is a need. [7]The high ionic conductivities of ionogel (IO) materials make them highly interesting for the fabrication of safer and lighter solid state gas sensor devices. Based on this approach, 1-ethyl-3-methylimidazolium bis(trifluoromethylsulfonyl)-imide([C2mim][TFSI]) IL immobilized in a polyurethane matrix was tested against different VOCs in N2[10]. The IO displayed an accurate baseline recovery and a low signal to noise ratio. Sensitivity levels of 10, 6, 6, 8, and 2% were measured when tested against 1000 ppm of toluene, hexane, propanal, ethanol, and acetone vapors, respectively. Moreover, 1-butyl-3-methylimidazolium hexafluorophosphate ([BMI][PF6]) IL was incorporated to nanofibers of styrene-acrylonitrile [11]and nylon-6,6 [12]. Both systems were tested in air against different alcohols (22.0–276.1 ppm), THF (707.4 ppm) or ace-tone (904.5 ppm) vapors, showing good reversible responses and low recovery times. Despite the importance of measuringC6H6and HCHO in air at room temperature, to the best of our knowledge, no studies on IOs as sensing surfaces have been reported so far. Recently, it has been demonstrated an in situ method to encapsulate 1-ethyl-3-methylimidazolium ethyl sulfate([C2mim][EtSO4]) ionic liquid in a polymeric matrix of poly(N-isopropylacrylamide) (pNIPAAM) onto gold or AZO-interdigitated electrodes [13]. By means of electro-chemical impedance spectroscopy (EIS) the charge-transfer resistance of the IOs can be correlated with thetime necessary for the formation of the network during the photopolymerization process. The resulting film presents a homogeneous morphology [14] with a controlled cover-age of the metal electrodes. The excellent electrical con-tact between the IO and the sensing electrode has been proven by monitoring morphology

changes caused by an external stimulus [15]. Moreover, the presence of the polymeric matrix protects the IL from moisture making it suitable for to normal ambient conditions [16].In this work, we report the use of a IO gas sensor consisting of a [C2mim][EtSO4] IL immobilized in a pNIPAAM matrix for the detection of common air pollutants such as C6H6andHCHO at room temperature. The film sensor is integrated onto interdigitated electrodes, and its sensing performance was investigated in the presence of two carrier gases and com-pared with the neat IL. As a result, the sensor exhibited remarkable performances of high sensitivity, fast response/recovery times, and good stability towards gas detection at room temperature.

Experimental section

Reagents and materials

N-isopropylacrylamide, N,N′-methylene-bis(acrylamide), 2,2-imethoxy-2 phenylacetophenone, and the ionic liquid (IL) 1-ethyl-3-methylimidazolium ethyl sulfate were purchased from Sigma-Aldrich. Cyclic olefin copolymer (COP) was provided by Zeonex/Zeonor and pressure sensitive adhesive (PSA) was gently provided by Adhesive Research, Ireland. The masks used for the photolithographic process were manufactured by Microlithographic Services. For the photolithography process, Microposit S1818 G2 positive photoresist was purchased from Chemplate Materials. For the gas test, certified bottles of 99.9% C6H6or HCHO provided by Air Liquide, Spain were used.

Synthesis of the ionogel

The synthesis of the IO is based on our previously reported publication [17]. In brief, a mixture of N-isopropylacrylamide(7.99 mmol),N,N′-methylene-bis(acrylamide) (0.162 mmol) and the photoinitiator (2,2-dimethoxy-2-phenylacetophenone)was dissolved in 2 mL of [C2mim][EtSO4] IL. The reaction mixture was placed in a beaker and heated at 80 °C during 30 min. The chemical structure of the IO used in this study is shown in Fig.1. The details of the fabrication [18, 19] of the electrochemical device and integration with the IO have been included in the SI.

Measurement of the gas sensor response

The electrode with the photopolymerized IO was welded to a custom-made PCB and mounted in a sealed aluminium chamber. A mass flow measurement system was used to control the addition of gas in the chamber. It employs a PC with tailored National Instruments LabView software to control mass flow controllers (MFCs) from Bronkhorst Hi-Tech. The MFCs are devices used to measure and control the flow of fluids and gases. The MFCs can give a set point from 0 to 100%, and the device will control the rate off low to the given set point. Each gas line is connected to the corresponding gas bottle, and the concentration of the gas in the chamber is controlled by the MFC of that line. The at-mosphere consists of different concentrations of benzene or formaldehyde using either air or N2as a gas carrier. A total flow of 400 sccm was kept constant among measurements and pulses of 15 min of each gas were tested. To measure the sensor response a Keythley 2000 multimeter was connected to the sensor. The multimeter automatically uses the Auto range mode to adjust to the best range of current. The scheme of the system is depicted in Fig.1. To avoid variations between electrodes, the normalized sensor response(SR) was calculated using the following Eq.1SR %ðÞ¼R−R0=R0ðÞ 100ð1ÞwhereRis the resistance of the IO or IL under the target gasandR0is the resistance of the IO or IL exposed to the carrier gas. The relative

humidity and the temperature of the laboratory were measured with the Thermo-Hydrograph OPUS10 and values of 51 ± 4% and 22 ± 1 °C were obtained, respectively.

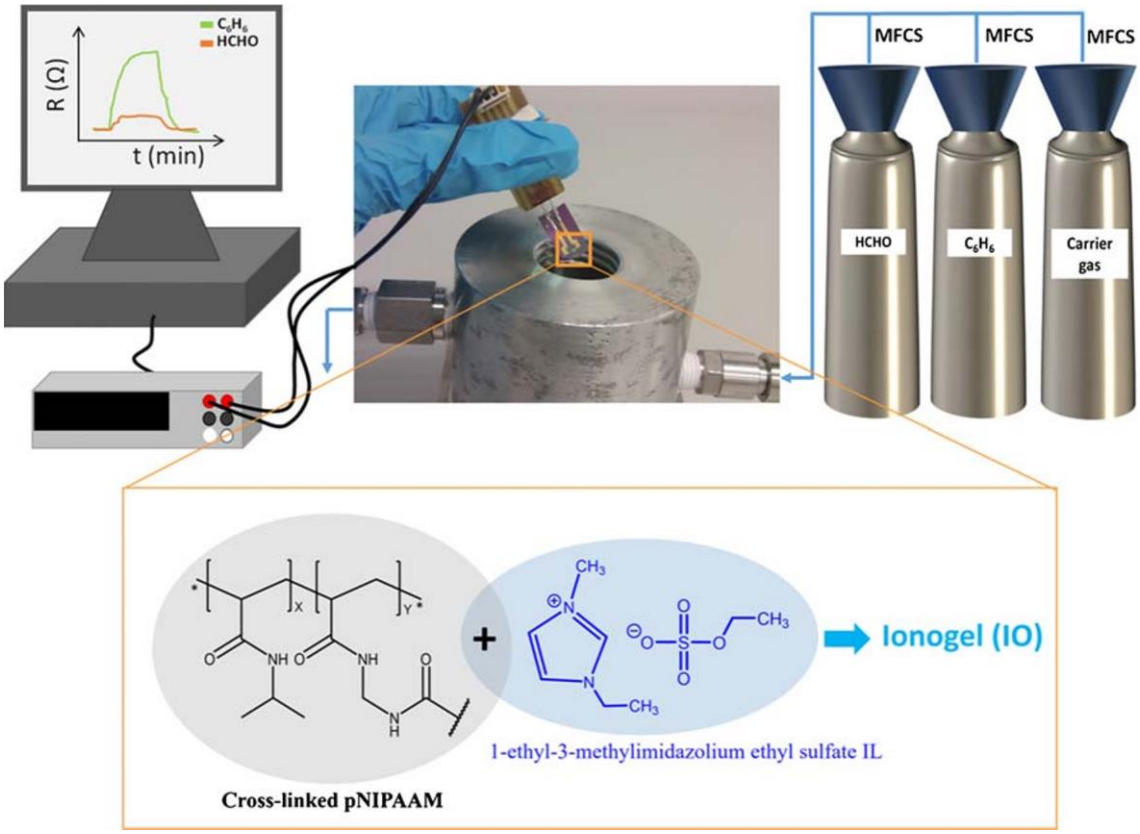

Fig. 1 Schematic illustration of the custom made system employed for the gas measurements of HCHO and C6H6 (top) and chemical structure of the material employed as a sensing layer (bottom). MFCS =mass flow control.

Results and discussion

The baseline of the gas sensor was obtained at room temperature by measuring the resistance between the two interdigitated electrodes against N2 as carrier gas. Once the stabilization of the baseline was achieved, the system was exposed to a gas pulse, and the variation on the resistance values over time was recorded. Figure 2 shows the SR of the IL (Fig. 2a) and the IO (Fig. 2b) against HCHO in N2, at different concentrations ranging from 10 to 50 ppm. The baseline has been corrected to facilitate comparisons between them. The corresponding plots without correction have been added in the supporting information. As can be seen in Fig. S1, the baselines of both materials present a drift towards higher resistance which could be produced by the adsorption of anions and/or cations at the IL-metal surfaces [16]. As a consequence, the number of ions responsible for charge transport is reduced, increasing the baseline resistance. Interestingly, this effect is minimized when the IL is encapsulated in the polymer matrix as an IO.

When the sensor is exposed to HCHO, an increase on the response of both materials was observed, and once the target gas flow was shut off, the resistance decreased showing a reversible behavior with a very stable response (see Fig. 2 a and b). The sensing mechanism is based on the miscibility of the gas in the IL, which is extremely complex since it depends on a variety of interactions that can simultaneously occur in an IL-gas system (dipole induction, dipole orientation or hydrogen-bonding interactions).

[20] These interactions will affect the physicochemical properties of the IL. Among others, viscosity changes are one of the most relevant factors to be considered since it is inversely proportional to the ionic conductivity [21]. For this reason, the conductivity of the IO based device can increase or decrease depending on the dominant molecular-ion interaction between the gas molecules and the ions of the IL. It has been reported an increase in conductivity of ILs or IOs upon exposing to VOCs such as hexane, ethyl acetate, dichloromethane, methanol, ethanol, methyl ethyl ketone, toluene, or trichloroethylene. The absorbed organic molecules become an additional path for ion migration [12] or decrease viscosity enhancing ion mobility [22, 23]. On the contrary, a decrease in conductivity proportional to the CO2 concentration has been reported for Ersoez et al. [24, 25] when testing an IO that contains 1-ethyl-3-methyl-imidazolium tetrafluoroborate ([EMIM][BF4]) as IL and polyvinylidene fluoridecohexafluoro propylene (PVDF-HFP) as polymer [26]. In our study, HCHO was introduced in the chamber and the gas molecules interacted with the IL ions increasing the resistance of the IO-HCHO and IL-HCHO systems. Different interactions can take place between HCHO and the ions. For instance, the alkyl groups of the IL ions could contribute to the dispersion interactions or to ion-dipole interactions originated between gas molecules and ions [27]. Those interactions could be responsible for an increase on the IO or IL viscosity, decreasing ion mobility and consequently, increasing resistance values. Before introducing the VOC, the mobility of the ions is induced by the voltage applied between the electrodes, and it is influenced by the presence of the carrier gas. After the introduction of the target gas, the gas molecules fill the polymer pores interacting with the ions, hindering their mobility and consequently increasing the resistance of the system.

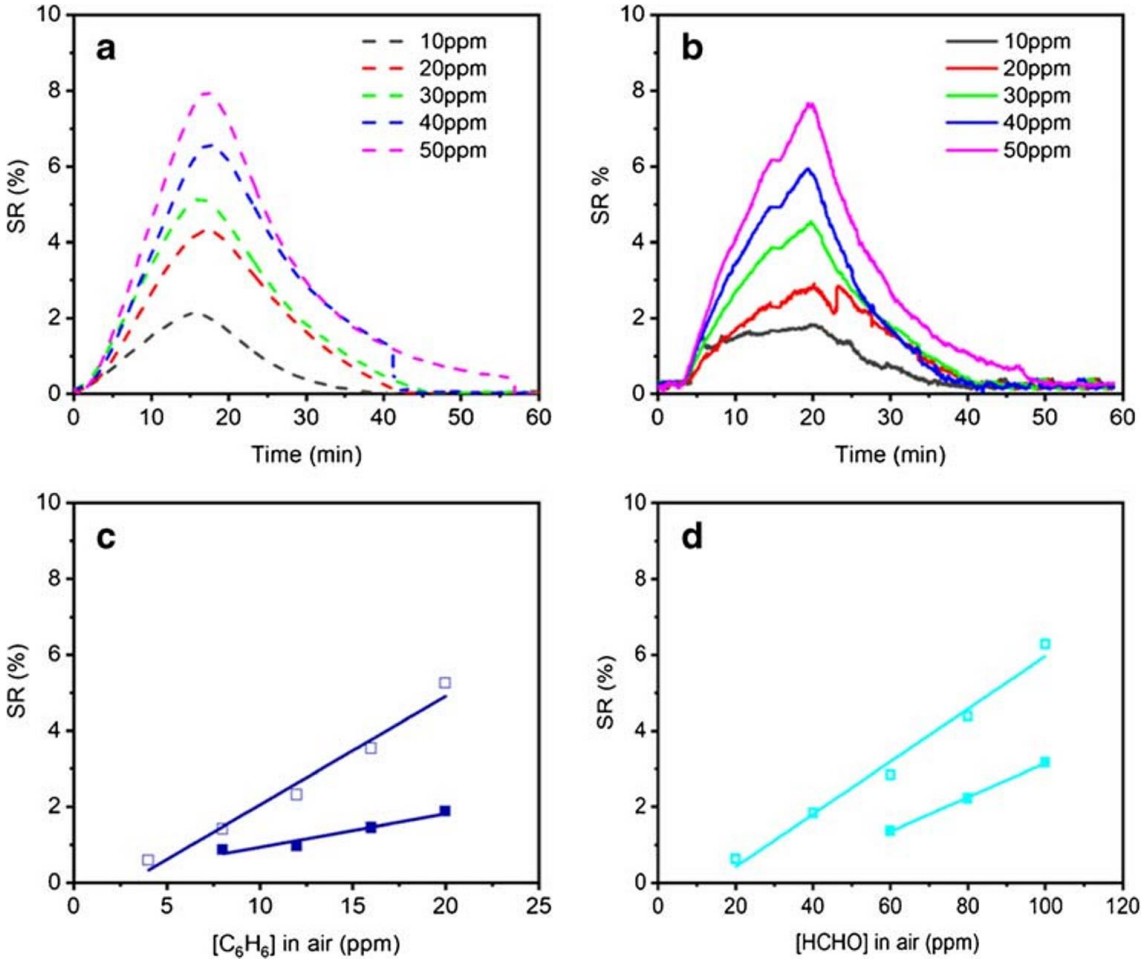

Fig. 2 IL (▪) (a) and IO (▫) (b) normalized responses to 10 ppm, 20 ppm, 30 ppm, 40 ppm, and 50 ppm of formaldehyde, employing N2 as carrier gas. Plot of the normalized sensor response of IL (▪) (a) and IO (▫) (b) as a function of the HCHO concentration diluted in N2 (c) or synthetic air (d), at 22 °C. All baselines were corrected.

The SR values obtained for both materials in N2 are similar and the change of the measured signal per HCHO concentration unit was calculated from the slopes of the Fig. 2c. The linear regression of the measured points shows a linear response for both materials with regression coefficients (R2) close to 0.9 values, indicating a good fit (see Table 1). The sensitivities presented similar values for the IO and IL (see Table 1 entry 1 and 2) indicating that there is no effect on sensitivity generated by the polymer matrix, when sensing HCHO in N2. The detailed response obtained for the IO and the corresponding neat IL sensors against a 15 min pulse of 30 ppm of HCHO using N2 as a carrier gas is presented in Fig. S2. When the sensor is exposed to HCHO, an increase on the response of both materials was observed, and once the target gas emission was shut off, the SR of IO immediately decreased showing a faster reversible behavior. In the case of the IL, the resistance increased during 3 min after shutting off the HCHO emission and then decreased. It is important to point out that this effect was not observed in every pulse, suggesting that the high viscosity of the raw IL (96.6 mPa s) [28] is most likely the responsible of this effect. The high viscosity of the IL results in a slow and less reproducible response, due to ion-pair formation [29]. In any case, this effect was not observed with the IO, which means that the porous polymer matrix circumvents the high viscosity of the IL.

To study the influence of the carrier gas, the experiment was repeated using HCHO diluted with synthetic air. The SR of the IO and IL are plotted in the Fig. S3c and S3d, respectively. No resistance change was observed for 20 ppm and 40 ppm of HCHO concentrations when the system was tested with the neat IL, which means that the IL does not interact with the gas at concentrations smaller than 60 ppm. In addition, the lower response of IL to HCHO in air and the better stabilization of the baseline for the IO confirm the protective role of the polymeric matrix. The calculated sensitivities for the IL and the IO are listed in Table 1 (entry 3 and 4). When N2 is used as carrier gas (Table 1 entry 1 and 2), it can be observed that the sensitivity to HCHO is one order of magnitude higher than the recorded when air is employed as a carrier gas. O2 solubility in ILs is better than that of N2 at the same temperature and pressure. [30] Therefore, we hypothesized that O2 adsorbed from the carrier gas could interfere in the gas sensing process, decreasing sensor response towards HCHO. The repeatability on the resistance response is an important characteristic to consider when developing gas sensors devices. In order to investigate this, the sensing layer was repeatedly exposed to HCHO in air at different concentration ranges (see Fig. S4). The coefficient of variation (CV) was calculated after three experiments to express the repeatability of the assay. CV values lower than 15% were obtained for 20, 40, 60, 80, and 100 ppm, respectively. The data show a slightly dispersion of the measurements in all cases, indicating a low variability response upon gas sensing sampling.

Table 1 Sensing gas, carrier gas, sensitivity, and R2 obtained when increasing gas concentrations.

Entry	Sensing material	Sensing gas	Carrier gas	Sensitivity[a]	R^{2}[b]
1	IO	HCHO	N_2	$(1.46 \pm 0.01) \times 10^{-3}$	0.994
2	IL	HCHO	N_2	$(1.39 \pm 0.10) \times 10^{-3}$	0.983
3	IO	HCHO	Air	$(0.65 \pm 0.05) \times 10^{-3}$	0.984
4	IL	HCHO	Air	$(0.45 \pm 0.01) \times 10^{-3}$	0.999
5	IO	C_6H_6	Air	$(2.48 \pm 0.26) \times 10^{-3}$	0.957
6	IL	C_6H_6	Air	$(0.88 \pm 0.01) \times 10^{-3}$	0.945

[a] Sensitivity (ppm^{-1}) of the sensor calculated from the slope of the linear regression; [b] Regression coefficient

The responses of the sensor against C6H6 diluted in air were also tested (see Fig. 3 a and b). In this case, the IO and IL responses were remarkably different. Apart from its higher response, the IO presents higher sensitivity than the IL (Fig. 3c and Table 1). The IL hardly responds to C6H6 in air. On the other hand, the IO presented an enhanced response to C6H6 since the amount of IL in the IO is much less than the amount of neat IL in a droplet. It has been reported [22] that, when the ILs are confined in a nanoscale space, as in the case of IOs, the gel network promotes the capture and concentration of gas molecules. Therefore, the physical properties of ILs become more sensitive to environmental stimuli. Besides, the sensor with IO as sensitive layer showed better stability of the baseline (see Fig. S5a and S5b) than the sensor with pure IL. The fluidic nature of IL could result in a continuous change of the shape of the drop during the experiment originating the instability of the baseline. Therefore, it can be concluded that the immobilization of the IL in pNIPAAM leads to an IO with aquasi-solid state that mitigates these variations and avoids IL leakage, resulting in a more robust and easier to handle sensor that was able to respond after 12 h of continuous measurements. The repeatability of the sensor with the IO was also evaluated (Fig. S6) and after 3 measurements CV values lower than 11% were obtained for all range of concentrations studied. These results are indicative of a very low dispersion of the measurements, proving a low variability between the experiments, except for the case of 4 ppm where the sensor is able to respond but with higher variability.

IO sensitivity towards C6H6 is higher than towards HCHO. These differences can be explained considering the molecular interactions between the ions of the IL and the VOCs and the solubility of the gases in ILs. The gas molecule-IL ion interaction is dominant, thus, it is responsible for the final performance of the sensitive material. C6H6 is a nonpolar molecule; therefore, it can be accommodated in the nonpolar region of the alkyl side chains of the IL. Moreover, it is expected to be miscible also in polar solvents that present a ring in their geometry, as is the case of the imidazolium cation, due to its quadrupole moment and planar structure with π-π interactions[31]. Therefore, the ring structure of imidazolium cation of the IL enhances the interaction with C6H6 molecules resulting in a stronger affinity towards C6H6. The LOD and the LOQ have been calculated for HCHO and C6H6. Lower LOD for C6H6 (LOD = 47 ppb) than for HCHO (LOD = 113 ppb) were obtained, which are below the standard permitted concentrations set by the WHO. The LOQ values were 157 ppb and 376 ppb for HCHO and C6H6 in air, respectively.

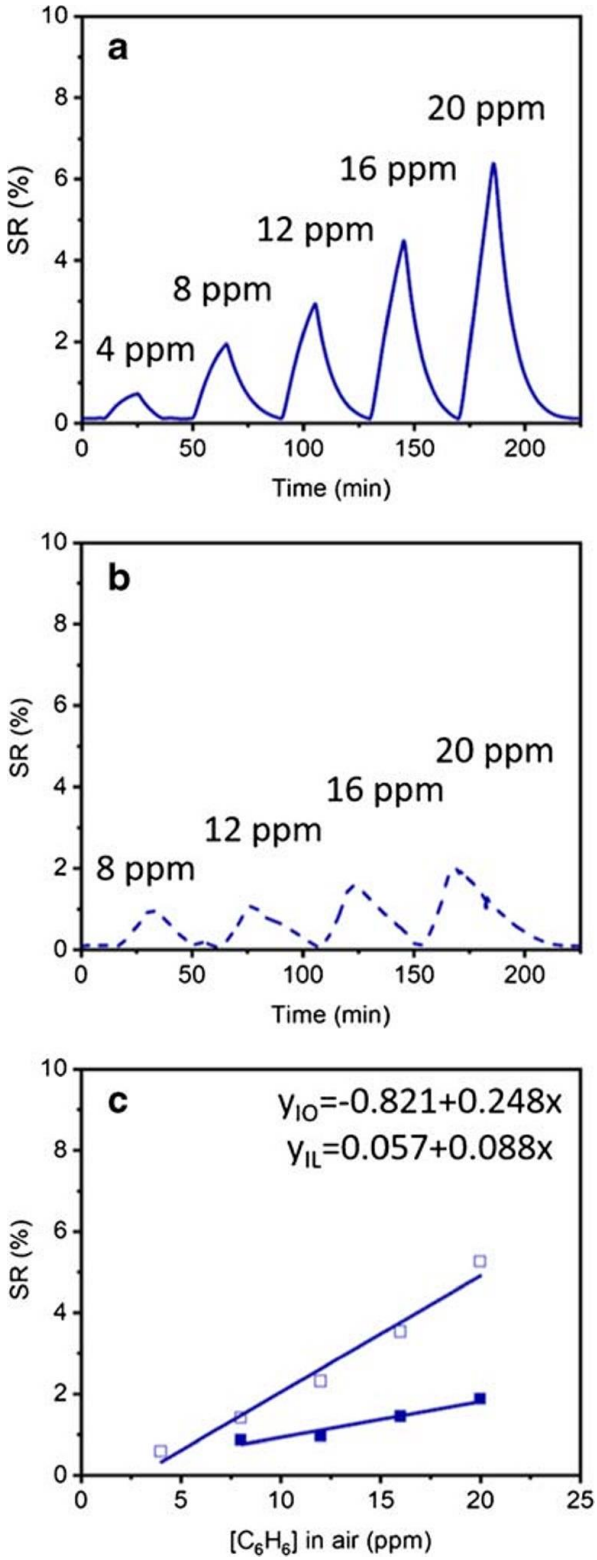

Fig. 3 a IO (▫) and b IL (▪) normalized responses to different concentrations of benzene in air. Room temperature normalized sensor response of the IO (▫) and the IL (▪) sensing layer as a function of C6H6 concentration diluted in air. All baselines were corrected.

Selectivity is defined as the ability of the sensor to respond in a selective manner to a specific group of analytes. The selectivity of this type of system is due to the employed IL that governs the adsorption of the gases in a selective manner. To prove this, a gas sensing film was prepared by encapsulating trihexyltetradecyl-phosphonium

dicyanamide IL (IL-2) in the pNIPAAM matrix. The sensing response of the neat IL and the IO is presented in Fig. S7. As can be seen in the figure, the phosphonium-based IL does not respond to any concentration of HCHO nor C6H6 demonstrating the selectivity of the imidazole-based IL towards the two tested gases. Water is also one of the best known interferes of ILs. Therefore, the effect of the humidity has been studied and is shown in Fig. S8. As can be seen, the changes in resistance are negligible for the tested relative humidity. This effect is in agreement with the low diffusion values measured for the IL when it is encapsulated in the polymeric matrix [16] corroborating the protective role of the pNIPAAM without the need of using hydrophobic or highly viscous anions. In addition, the use of the IL overcome the limitations of the traditional gas sensors towards hot and dry environments since do not suffer evaporation effects like water or organic containing simplifying the sensor design.

The response (t90) and recovery times (tr90) were calculated for HCHO and C6H6 in air. t90 is defined as the time to achieve 90% of the overall signal change and tr90 the time necessary to return to 90% of the value read prior to exposure. t90 and tr90 were calculated after stabilization of 10 ppm of the target gases, see Fig. 4. It is important to point out that no stabilization was achieved with the IL sensors. With IO, a t90 of 12 min and a tr90 of 11 min were obtained for HCHO in air. In the case of C6H6 pulse, t90 and tr90 of 25 min and 21 min were calculated for the same concentration. The thick film of IO employed in the sensing device could be responsible for the high t90 and tr90 values. Since the photopolymerization of the IO was carried out in situ onto the electrodes, a film of around 1 mm in thickness was obtained in contrast to the usually employed films of 1 μm found in the literature [24]. This thick layer would slow down the diffusion of the gas molecules. Moreover, as can be observed, faster response and recovery times were obtained when testing HCHO than when testing C6H6. The faster response- and recovery-times of HCHO could be correlated with molecular weight of the tested molecules, those with large molecules (C6H6) exhibit slower dynamics [32].

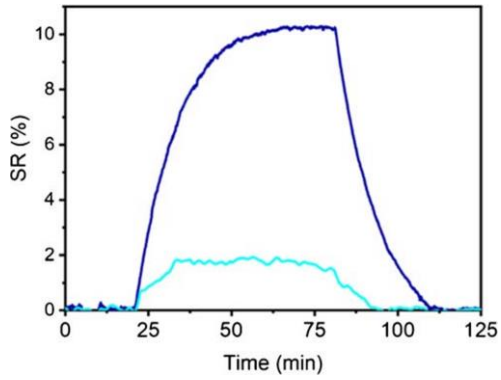

Fig. 4 Response of the IO for a 10 ppmconcentration of C6H6 (dark blue) and HCHO (cyan) diluted in synthetic air at room temperature. Both baselines were corrected.

Conclusions

In this work, the viability of using an IO for the detection of two VOCs at room temperature is demonstrated. For this purpose, [C2mim][EtSO4] IL has been encapsulated into a pNIPAAM matrix and the resistance changes against C6H6 and HCHO diluted in either N2 or synthetic air are studied at different concentrations. IO presented a positive response towards both VOCs showing good reversibility at room temperature. The stronger affinity of IO to C6H6, due to the interactions between imidazolium cations and C6H6 molecules, resulted in higher sensitivity and lower LOD. In addition, a possible interference of the oxygen from the carrier gas was suggested since, HCHO diluted in

N2 presented better sensitivity than when synthetic air was used as carrier gas. Moreover, a better understanding of the matrix effect on these types of sensors is provided. The sensitivities of the IO were compared with those of pure IL achieving higher values when sensing C6H6 with the IO. Furthermore, the polymer matrix protects the IL from the water humidity and mitigates adsorption of anions or cations at the IO-electrified metal surface resulting in more stable responses. This paper represents several advances in the field of gas sensors at room temperature. Without the need to use heating, a time and cost reduction are achieved comparing with other methods, such as semiconductor deposition. To further improve the use of the sensor in commercial application, a wider screening of ILs should be performed to find the most suitable for each VOC and combined with principal analysis components (PCA). This work contributes to widening the use of IOs for air monitoring, for instance, in synthetic products as paints and waxes storage rooms, working environments like chemical industries and laboratories, at home, for air quality control or in dry or hot ambient where conventional liquid electrolytes suffer from evaporation.

Acknowledgments

This work was supported by the Ministry of Economy and Competitiveness (MINECO) of Spain under the TEMIN-++AIR programs. N.G.-G. was supported by a PhD fellowship from the University of Navarra. F. B.-L. acknowledges the funding support from Gobierno de España, Ministerio de Economía y Competitividad, with Grant No. BIO2016-80417-P, and Gobierno Vasco Dpto. Educación for the consolidation of the research groups (IT1271-19).

References

1. Khan FI, Ghoshal AK (2000) Removal of volatile organic compounds from polluted air. J Loss Prev Process Ind 13:527–545. https://doi.org/10.1016/S0950-4230(00)00007-3
2. Schiavon M, Redivo M, Antonacci G, Rada EC, Ragazzi M, Zardi D, Giovannini L (2015) Assessing the air quality impact of nitrogen oxides and benzene from road traffic and domestic heating and the associated cancer risk in an urban area of Verona (Italy). Atmos Environ 120:234–243. https://doi.org/10.1016/j.atmosenv.2015.08.054
3. (2010) World Health Organization. Regional Office for Europe. WHO guidelines for air quality
4. Jalal AH, Alam F, Roychoudhury S, Umasankar Y, Pala N, Bhansali S (2018) Prospects and challenges of volatile organic compound sensors in human healthcare. ACS Sensors 3:1246–1263
5. Chatterjee S, Castro M, Feller JF (2015) Tailoring selectivity of sprayed carbon nanotube sensors (CNT) towards volatile organic compounds (VOC) with surfactants. Sensors Actuators B Chem 220:840–849. https://doi.org/10.1016/j.snb.2015.06.005
6. Zhang J, Qin Z, Zeng D, Xie C (2017) Metal-oxide-semiconductor based gas sensors: screening, preparation, and integration. Phys Chem Chem Phys 19:6313–6329. https://doi.org/10.1039/c6cp07799d
7. Bai H, Shi G (2007) Gas sensors based on conducting polymers. Sensors 7:267–307. https://doi.org/10.3390/s7030267
8. Rojo L, Castro-Hurtado I, Mandayo GG, Castaño E, Morant-Miñana MC (2017) Thin-film potentiometric sensor to detect

CO2 concentrations ranging between 2% and 100%. Electroanalysis 29:2358–2364. https://doi.org/10.1002/elan.201700304
9. Liu X, Cheng S, Liu H, Hu S, Zhang D, NingH (2012) A survey on gas sensing technology. Sensors 12:9635–9665. https://doi.org/10.3390/s120709635

10. Jin ML, Park S, Kim J-S, Kwon SH, Zhang S, Yoo MS, Jang S, Koh HJ, Cho SY, Kim SY, Ahn CW, Cho K, Lee SG, Kim DH, Jung HT (2018) An ultrastable ionic chemiresistor skin with an intrinsically stretchable polymer electrolyte. Adv Mater 30: 1706851. https://doi.org/10.1002/adma.201706851
11. Kim M, Kang E, Park DW et al (2012) Ionic liquid/styreneacrylonitrile copolymer nanofibers as chemiresistor for alcohol vapours. Bull Kor Chem Soc 33:2867–2872. https://doi.org/10.5012/bkcs.2012.33.9.2867
12. Kang E, Kim M, Oh JS, Park DW, Shim SE (2012) Electrospun BMIMPF6/Nylon 6,6 nanofiber chemiresistors as organic vapour sensors. Macromol Res 20:372–378. https://doi.org/10.1007/s13233-012-0043-0
13. Gil-González N, Chen C, Akyazi T, Zuzuarregui A, Rodriguez A, Knez M, Castaño E, Benito-Lopez F, Morant-Miñana MC (2018) AZO embedded interdigitated electrodes for monitoring stimuli responsive materials. Adv Funct Mater 28:1803127
14. Akyazi T, Gil-González N, Basabe-Desmonts L, Castaño E, Morant-Miñana MC, Benito-Lopez F (2017) Manipulation of fluid flow direction in microfluidic paper-based analytical devices with an ionogel negative passive pump. Sensors Actuators B Chem 247: 114–123. https://doi.org/10.1016/j.snb.2017.02.180
15. Gil-González N, Akyazi T, Castaño E, Benito-Lopez F, Morant-Miñana MC (2018) Elucidating the role of the ionic liquid in the actuation behavior of thermo-responsive ionogels. Sensors Actuators B Chem 260:380–387. https://doi.org/10.1016/j.snb.2017.12.153
16. Gil-González N, Benito-Lopez F, Castaño E, Morant-Miñana MC (2020) Electrical and electrochemical properties of imidazolium and phosphonium-based pNIPAAM ionogels. Electrochim Acta 345. https://doi.org/10.1016/j.electacta.2020.136167
17. Akyazi T, Saez J, Elizalde J, Benito-Lopez F (2016) Fluidic flow delay by ionogel passive pumps in microfluidic paper-based analytical devices. Sensors Actuators B Chem 233:402–408. https://doi.org/10.1016/j.snb.2016.04.116
18. Rojo L, Castro-Hurtado I, Morant-Miñana MC, Mandayo GG, Castaño E (2014) Li2CO3 thin films fabricated by sputtering techniques: the role of temperature on their properties. CrystEngComm 16:6033–6038. https://doi.org/10.1039/b000000x
19. Rojo L, Castro-Hurtado I, Morant-Miñana MC, Mandayo GG, Castaño E (2015) Enhanced features of Li2CO3 sputtered thin films induced by thickness and annealing time. CrystEngComm 17: 1597–1602
20. Liang C, Yuan C-Y, Warmack RJ, Barnes CE, Dai S (2002) Ionic liquids: a new class of sensing materials for detection of organic vapors based on the use of a quartz crystal microbalance. Anal Chem 74:2172–2176. https://doi.org/10.1021/ac011007h
21. Southall JP, Hubbard HVSA, Johnston SF et al (1996) Ionic conductivity and viscosity correlations in liquid electrolytes for incorporation into PVDF gel electrolytes. Solid State Ionics 85:51–60
22. Zhu X, Zhang H,Wu J (2014) Chemiresistive ionogel sensor array for the detection and discrimination of volatile organic vapor. Sensors Actuators B Chem 202:105–113. https://doi.org/10.1016/j.snb.2014.05.075
23. Hussain A, Semeano ATS, Palma SICJ, Pina AS, Almeida J, Medrado BF, Pádua ACCS, Carvalho AL, Dionísio M, Li RWC, Gamboa H, Ulijn RV, Gruber J, Roque ACA (2017) Tunable gas sensing gels by cooperative assembly. Adv Funct Mater 27: 1700803. https://doi.org/10.1002/adfm.201700803
24. Ersoez B, Bauersfeld M-L, Wöllenstein J (2016) Ionogel—based composite material for CO2 sensing deposited on a chemiresistive transducer. Proceedings 1:314. https://doi.org/10.3390/proceedings1040314
25. Ersöz B, Schmitt K,Wöllenstein J (2020) Electrolyte-gated transistor for CO2 gas detection at room temperature. Sensors Actuators B Chem 317:128201. https://doi.org/10.1016/j.snb.2020.128201
26. Ishizu K, Takei Y, HondaMet al (2013) Carbon dioxide gas sensor with ionic gel. 2013 Transducers Eurosensors XXVII 17th Int Conf solid-state sensors. Actuators Microsyst Transducers Eurosensors 2013:1633–1636. https://doi.org/10.1109/Transducers.2013.6627097

27. Jin X, Yu L, Garcia D, Ren RX, Zeng X (2006) Ionic liquid hightemperature gas sensor array. Anal Chem 78:6980–6989. https://doi.org/10.1021/ac0608669
28. Arce A, Rodil E, Soto A (2006) Volumetric and viscosity study for the mixtures of 2-ethoxy-2-methylpropane, ethanol, and 1-ethyl-3-methylimidazolium ethyl sulfate ionic liquid. J Chem Eng Data 51: 1453–1457
29. Rehman A, Zeng X (2015) Methods and approaches of utilizing ionic liquids as gas sensing materials. RSC Adv 5:58371–58392. https://doi.org/10.1039/C5RA06754E
30. Zhigang L, Chengna D, Chen B (2014) Gas solubility in ionic liquids. Chem Rev 114:1289–1326
31. Núñez-Rojas E, Flores-Ruiz HM, Alejandre J (2018) Molecular dynamics simulations to separate benzene fromhydrocarbons using polar and ionic liquid solvents. J Mol Liq 249:591–599. https://doi.org/10.1016/j.molliq.2017.10.147
32. Marešová E, Tomeček D, Fitl P, Vlček J, Novotný M, Fišer L, Havlová Š, Hozák P, Tudor A, Glennon T, Florea L, Coyle S, Diamond D, Skaličan Z, Hoskovcová M, Vrňata M (2018) Textile chemiresistors with sensitive layers based on polymer ionic liquids: applicability for detection of toxic gases and chemical warfare agents. Sensors Actuators B Chem 266:830–840. https://doi.org/10.1016/j.snb.2018.03.157